

Frequency comparison VM1 – NRC-Sr+1

For the period MJD 60999-61004

A frequency comparison of the $^{88}\text{Sr}^+$ secondary frequency standard NRC-Sr+1 (1780301) has been made with respect to the active hydrogen maser VM1 (1400307) during the measurement campaign of MJD 60999-61004. Tab. 1 below summarizes the result as well as the associated uncertainties.

Tab. 1: Summary of results

Evaluation period (MJD)	60999 – 61004
Fractional uptime	45.96%
$y(\text{VM1} - \text{Sr+1}) [10^{-15}]$	-129.9050
$u_A (1\sigma) [10^{-15}]$	0.0085
$u_B (1\sigma) [10^{-15}]$	0.0117
$u_{A,LAB} (1\sigma) [10^{-15}]$	0.20
$u_{B,LAB} (1\sigma) [10^{-15}]$	0
$u_{total} (1\sigma) [10^{-15}]$	0.20

Methods

The influence of systematic effects on the $^{88}\text{Sr}^+$ secondary frequency standard NRC-Sr+1 was investigated in [1, 2]. The effects for which NRC-Sr+1 is corrected are:

- blackbody radiation field
- thermal motion
- quadratic Zeeman shift
- collisional frequency shift
- 1092 nm ac Stark shift
- 674 nm ac Stark shift
- 422 nm ac Stark shift
- gravitational redshift

Several other systematic effects did not produce a measurable bias, but do contribute to the overall uncertainty of Sr+1 and are included in the uncertainty budget. A full uncertainty budget for Sr+1 for the evaluation period of MJD 60999 – 61004 is given in Tab. 2.

For this measurement, the $^{88}\text{Sr}^+$ secondary frequency standard was operated as in [2]. The ultra-stable 674 nm laser frequency was actively de-drifted using an acousto-optic modulator in a fiber-noise cancellation scheme (Fig. 1). The synthesizer was common to two fibre phase noise

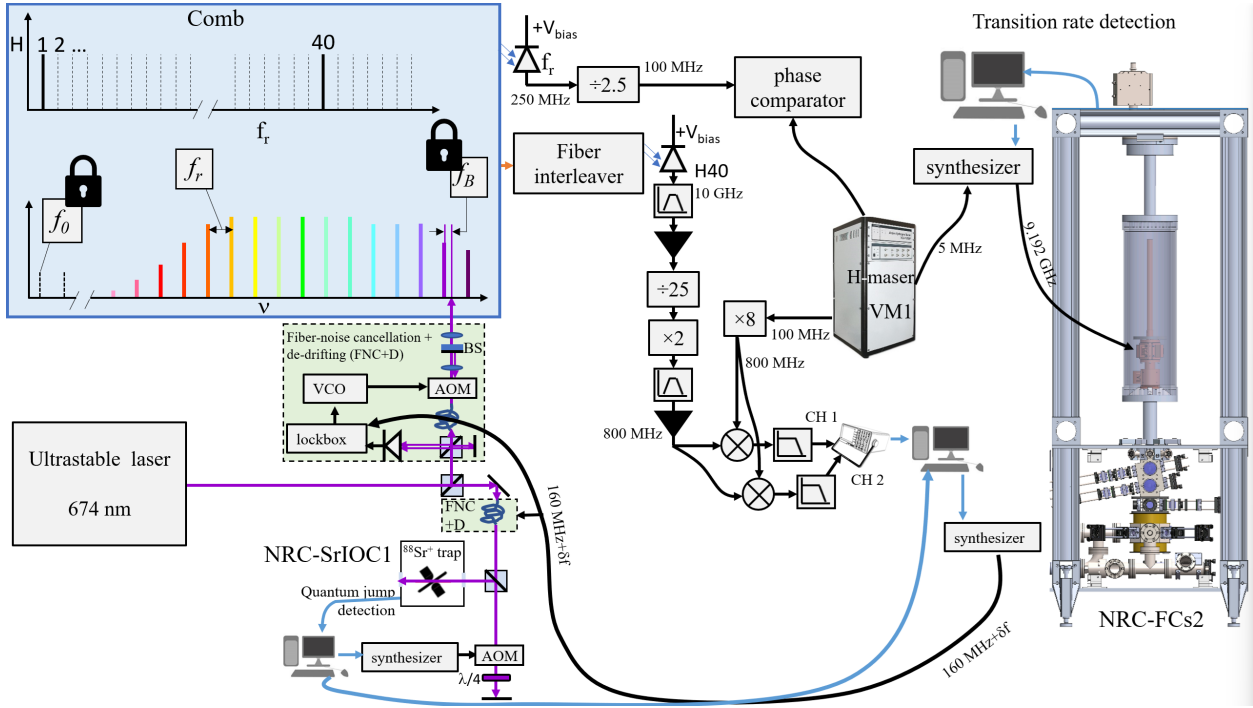


Fig. 1: Experimental setup. See text for details

cancellation arms, the frequency standard arm and the comb arm. The synthesizer was moving the lockpoint to keep constant the laser frequency reaching both the $^{88}\text{Sr}^+$ frequency standard and the frequency comb. The $^{88}\text{Sr}^+$ clock data itself was used to inform the de-drifting algorithm.

The comb, with a repetition rate of 250 MHz, was phase-locked to the 674 nm de-drifted probe laser. A commercial fiber interleaver module produced an ultrastable microwave signal at the 40th harmonic of the repetition rate (10 GHz). This signal was divided down by a digital prescaler (Centellax UXN40M7K) to 400 MHz and its second harmonic (800 MHz) was isolated by a band-pass filter. This 800 MHz signal, proportional to the comb repetition rate, was compared to the 8th harmonic of the VM1 100 MHz output in two different channels in near quadrature, ensuring that always at least one channel was in the linear region. The resulting voltage output of the double-balanced mixers was calibrated (to convert voltage into phase) and sampled every second by an oscilloscope. During the voltage to phase calibration, the comb was intentionally detuned from the nominal repetition rate (250 MHz) by a few mHz. The measured voltage followed a roughly sinusoidal shape as the relative phase at 800 MHz went through 2π radians in a few minutes. Linear interpolation from the calibration dataset was used to make the voltage to phase conversion as accurate as possible. A second method was also used to verify the phase comparison between the comb repetition rate and VM1. It used a commercial phase noise analyzer model 53100A from Microchip operating at 100 MHz. Both methods agree, with their difference well within the link uncertainty (Tab. 3).

The ion clock itself makes 30 interrogations of the ion 4-Hz-detuned from the centre of a specific transition of $^{88}\text{Sr}^+$ first on the red side, then on the blue side [2]. Interrogation pulses are 0.1 s each, and one spectroscopic transition is fully interrogated in 7.66 s. Three Zeeman pairs of spectroscopic transitions with line centre frequencies C_2, C_3 and C_4 were interrogated in total to cancel electric quadrupole shifts [3]. A complete clock cycle, therefore, lasts around 46 s. The $^{88}\text{Sr}^+$ clock measured the offset of the de-drifted probe laser to the centre of the electric-quadrupole-shift-removed transition.

For the analysis here, the $^{88}\text{Sr}^+$ clock data was binned in durations of 3365 s on average. The

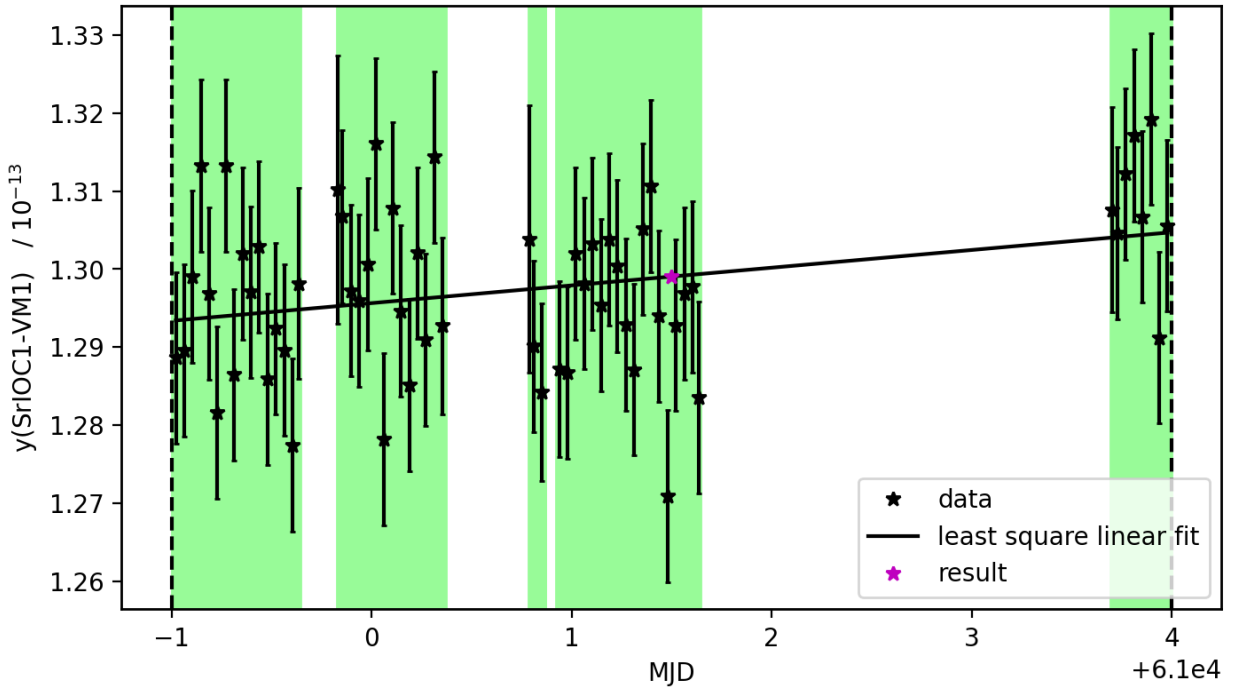


Fig. 2: $y(\text{Sr1-VM1})$. The up-time is the shaded green region. The linear fit and the result (magenta star) are also shown.

nominal frequency of the ion clock, after correcting for systematic effects, was assumed to be 444,779,044,095,486.3 Hz as per [4]. The fractional frequency difference $y(\text{VM1} - \text{Sr1})$ was calculated for every data bin. A linear regression, weighted by the time span of each bin, was used to determine the fractional frequency difference at the middle of the reporting period, MJD 61001.5 (see Fig. 2).

Uncertainties

Type A uncertainty

For this dataset, the long term stability of Sr+1 follows $\sigma_y = 3.8 \times 10^{-15} / \sqrt{\tau}$ where σ_y is the Allan deviation and τ is the averaging time. The reported value for type A uncertainty, u_A , is calculated from $u_A = 3.8 \times 10^{-15} / \sqrt{\tau} = 8.5 \times 10^{-18}$ where $\tau = 198536$ s is the averaging period. The Allan deviation plot of Sr+1, calculated using the procedure described in [5], is shown at Fig. 3.

Type B uncertainty

The exhaustive list is given in Tab. 2. The gravitational redshift of the clock has been corrected for the post-glacial rebound of Earth's crust measured at NRC (3.2 mm / year of positive vertical displacement) and for the optical clock height adjustment in the lab frame since the experiments in [1]. The black body radiation (BBR) shift given in Tab. 2 was calculated based on a model [6] and a measurement of the wall temperature using four thermistors. The wall temperature was averaged over the measurement up-time. The BBR coefficient and uncertainty were taken from [7].

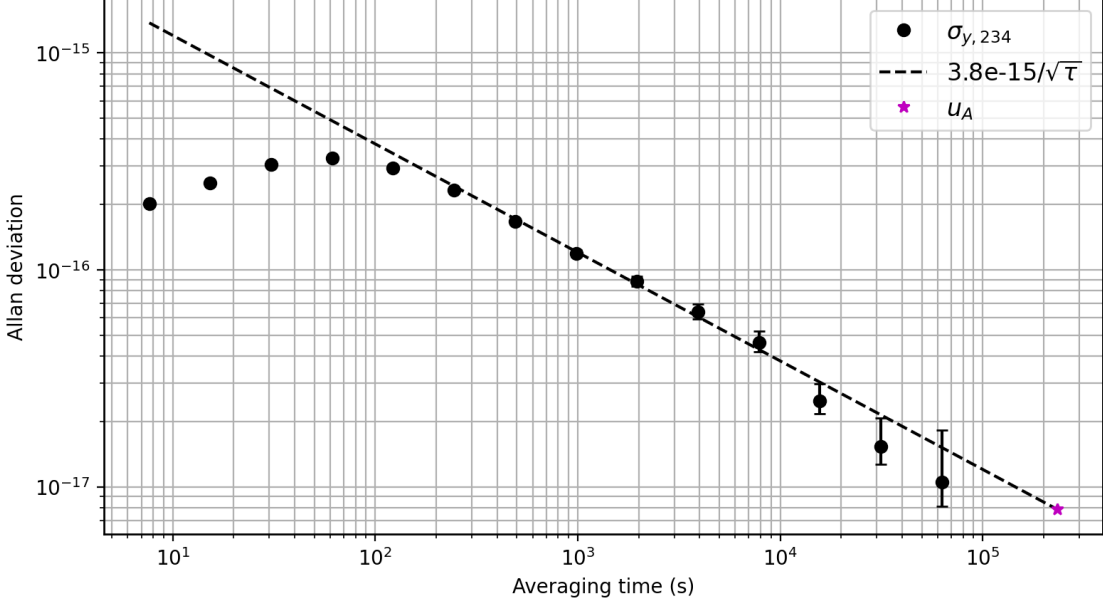


Fig. 3: NRC-Sr1+ Allan deviation over the whole data set. The overall fit is the black dashed line. See text for details.

Tab. 2: Uncertainty budget of NRC-Sr+1. All values are in fractional frequency units of 10^{-18} .

Source of shift	Shift	Uncertainty
BBR field evaluation, $\langle E^2 \rangle_T$	564.9	11
Collisional frequency shift	-0.045	2.6
BBR coefficient, $\Delta\alpha_0$	0	0.22
Thermal motion	-2.59	0.16
AOM chirps	0	0.4
Excess micromotion	0	0.54
Servo tracking errors	0	0.1
1092 nm ac Stark shift	-1	0.42
Electric quadrupole shift	0	0.03
674 nm ac Stark shift	0.036	0.02
422 nm ac Stark shift	0.006	0.006
Tensor Stark shift	0	0.005
Quadratic Zeeman shift	0.119	0.001
Total for Sr+1	561.4	11.4
Gravitational redshift	10453.5	2.6
Total	11015.0	11.7

Tab. 3: Link uncertainty budget of NRC-Sr+1. All values are in fractional frequency units of 10^{-15} .

Uncertainty Source	Uncertainty
Dead time	0.18
Frequency comb	0.07
Total	0.20

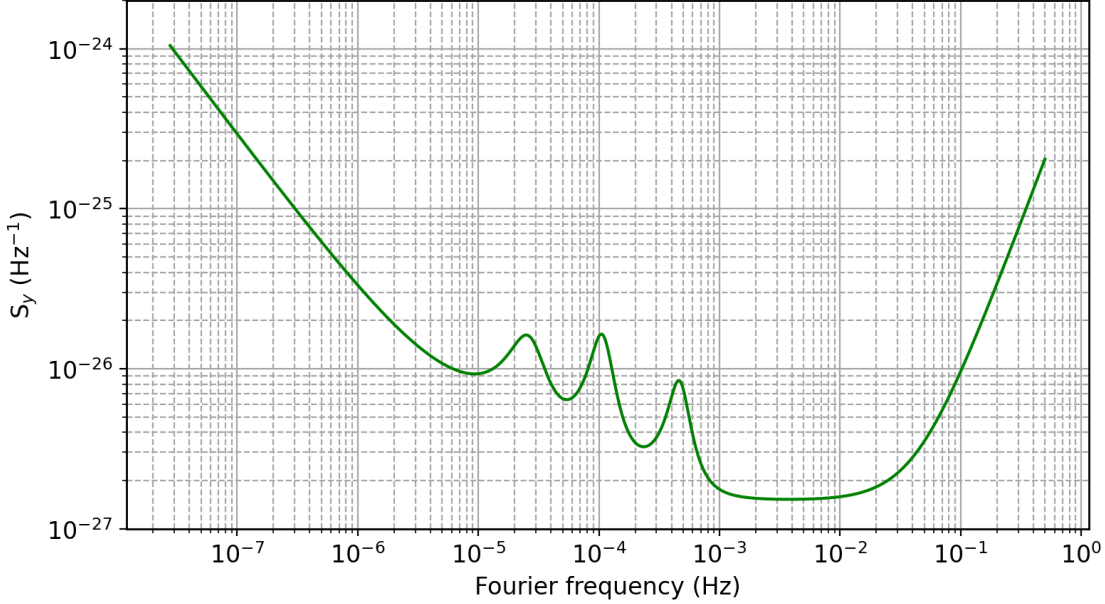


Fig. 4: VM1 maser phase noise model that fits the data of Fig. 5.

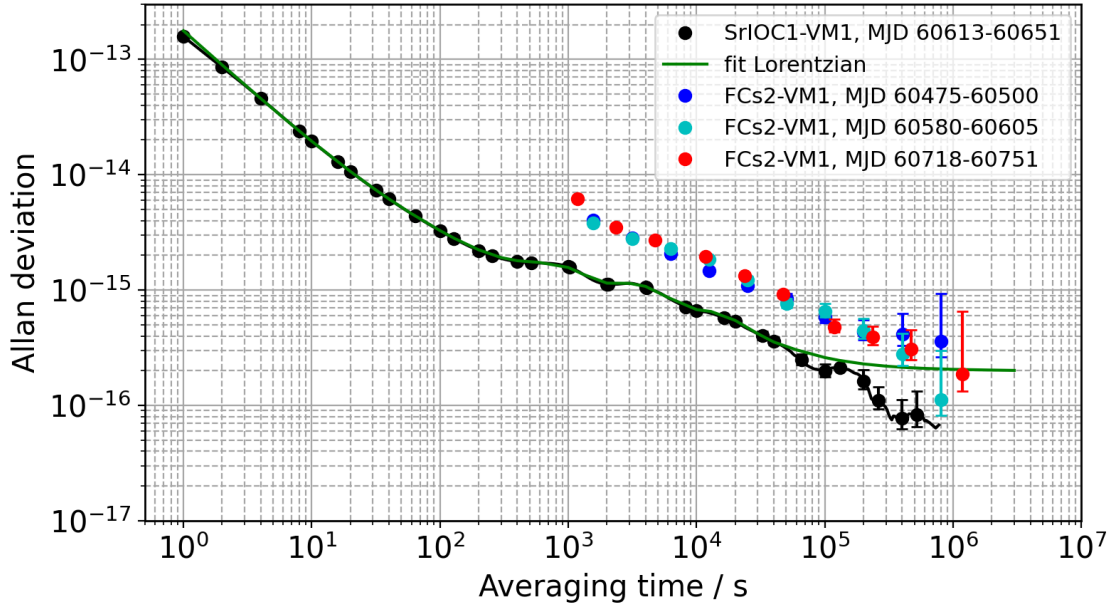


Fig. 5: Link uncertainty Allan deviation plots. The black circle dataset is the Allan deviation of the linearly dedrifted y (Sr+1-VM1) taken from our November-December 2024 measurement campaign [2]. The green line fit uses the model of Fig. 4. The blue and red circles are (linearly dedrifted) measurements [2] of VM1 using NRC-FCs2. They justify the long term flicker floor of 2×10^{-16} .

Link to local reference clock

The uncertainty of the link with our reference clock VM1, $u_{A,LAB}$, is the sum of two terms added in quadrature (Tab. 3). The first term, calculated following the procedure described in [1], is attributed to measurement dead time. It is calculated using the uptime distribution and a best fit model of the phase noise power spectral density of VM1 (Fig. 4). Fig. 5 shows the Allan deviation calculated from this best fit model of VM1 (green line). Fig. 5 also shows the Allan deviation of a dedrifted Sr+1-VM1 measurement from our November-December 2024 campaign [2]. The second term of the link uncertainty is an upper bound for the uncertainty of the optical frequency comb and it is modeled by $3 \times 10^{-14} / \sqrt{\tau}$. This value is derived from the NRC-FCs2 stability when it is operated simultaneously using the ultrastable microwaves generated from the same optical frequency comb.

References

- [1] B. Jian *et al.* (2023) *Metrologia* **60**, 015007.
- [2] C. Marceau *et al.* (2025) *Metrologia* **62**, 045001.
- [3] P. Dubé *et al.* (2005) *Phys. Rev. Lett.* **95**, 033001.
- [4] Consultative Committee for Time and Frequency 2021 Recommendation CCTF PSFS 2 (2021): updates to the CIPM list of standard frequencies (available at: www.bipm.org/en/committees/cc/cctf/22-2-2021).
- [5] P. Dubé *et al.* (2015) *Phys. Rev. A* **92**, 042119.
- [6] P. Dubé *et al.* (2013) *Phys. Rev. A* **87**, 023806.
- [7] T. Lindvall *et al.* (2025) *Phys. Rev. Lett.* **135**, 043402.